

See discussions, stats, and author profiles for this publication at: <https://www.researchgate.net/publication/231407861>

# Water in Silicate Glasses: Quantitation and Structural Studies by $^1\text{H}$ Solid Echo and MAS-NMR Methods

ARTICLE *in* THE JOURNAL OF PHYSICAL CHEMISTRY · APRIL 1988

Impact Factor: 2.78 · DOI: 10.1021/j100318a070

---

CITATIONS

179

---

READS

17

4 AUTHORS, INCLUDING:



[Hellmut Eckert](#)

University of Münster

536 PUBLICATIONS 9,053 CITATIONS

SEE PROFILE

# Water in Silicate Glasses: Quantitation and Structural Studies by $^1\text{H}$ Solid Echo and MAS-NMR Methods<sup>†</sup>

Hellmut Eckert,<sup>‡</sup> James P. Yesinowski,\*

Division of Chemistry and Chemical Engineering, California Institute of Technology,  
Pasadena, California 91125

Lynn A. Silver, and Edward M. Stolper

Division of Geological and Planetary Sciences, California Institute of Technology,  
Pasadena, California 91125 (Received: September 3, 1987)

$^1\text{H}$  wideline and magic angle spinning (MAS) NMR results are reported for water in a series of synthetic and naturally occurring silicate glasses containing from 0.04 to 9.4 wt %  $\text{H}_2\text{O}$ . For glasses free of paramagnetic metal ions, the absolute water contents can be accurately determined by a solid echo  $^1\text{H}$  NMR technique with pyrophyllite,  $\text{Al}_2\text{Si}_4\text{O}_{10}(\text{OH})_2$ , as an intensity reference. The MAS-NMR spectra can be interpreted as superpositions of the individual spectra of OH and anisotropically constrained  $\text{H}_2\text{O}$  groups, the latter giving rise to spinning sidebands extending over ca. 100 kHz. Two methods are described to obtain percentages of OH and  $\text{H}_2\text{O}$  groups from the relative intensities of the centerband and the spinning sidebands in these glasses. The MAS-NMR results are consistent with previous IR analyses indicating that low levels of water (<2–4 wt %) are mainly present as OH groups whereas at higher concentrations molecular  $\text{H}_2\text{O}$  species dominate. Simulations of the MAS-NMR spectra based on the individual spectra of compounds in which the hydrogen-bearing species are structurally isolated (OH in tremolite and  $\text{H}_2\text{O}$  in analcite) accurately reproduce the experimental spectra, indicating that the OH or  $\text{H}_2\text{O}$  groups in the glasses are not preferentially clustered. The MAS-NMR centerband line shapes are dominated by a distribution of isotropic chemical shifts. The well-established linear dependence of  $^1\text{H}$  chemical shifts on the O—H...O distance (a measure of the hydrogen bonding strength) leads to average distances of  $290 \pm 1.5$  pm in all synthetic glasses except silica,  $293 \pm 1.5$  pm in the volcanic rhyolite glasses, and 298 pm in silica glass. This value does not depend on the total water contents, indicating that the hydrogen-bonding characteristics of OH and  $\text{H}_2\text{O}$  species in the glasses are similar. The  $^1\text{H}$  wideline NMR procedure above yields underestimates of the total water content for synthetic and volcanic glasses containing ca. 1 wt % iron, presumably due to extreme signal broadening by the strong dipolar fields from the electron spins of the paramagnetic ions. These dipolar couplings also affect the line shape of the observable portion of the hydrogen resonance and produce intense spinning sidebands in the MAS-NMR spectra which invalidate determinations of OH/ $\text{H}_2\text{O}$  ratios in these cases.

## Introduction

The state of water in oxide glasses has received considerable attention both in geology and in materials science.<sup>1</sup> Water plays a crucial role in modifying the phase equilibria and physical properties of magmas; hence much effort has been devoted to determining the concentration and speciation of water in volcanic glasses<sup>2</sup> and in synthetic analogues of magmas.<sup>3</sup> From a materials research standpoint, the presence of even minor amounts of water in silicate glass has been shown to alter drastically the physico-chemical properties and possible ranges of technological applications.<sup>4</sup> While the influence of water upon the macroscopic properties of silicate melts has been studied extensively,<sup>5,6</sup> direct structural information about the nature of hydrogen-bearing species and their bonding environments cannot be obtained readily from such measurements. Investigation of glasses quenched from melts is a frequent approach to answering these questions.<sup>7</sup> Recent studies of infrared overtone and combination bands<sup>1–3,7</sup> demonstrate that water in silicate glasses is present as OH and molecular  $\text{H}_2\text{O}$  groups. These studies suggest that low contents of water disrupt the glass network, transforming (Al,Si)—O—(Al,Si) linkages into (Al,Si)—OH bonds. Above ca. 2–4 wt %  $\text{H}_2\text{O}$  (depending on the glass composition) the number of hydroxyl groups thereby created levels off, and water enters the glass structure predominantly in the form of molecular species. The concentrations of these species as well as the absolute proton content of glasses determined by infrared spectroscopy have been shown to be compatible with a thermodynamic analysis of phase equilibrium data for hydrous silicate melts.<sup>3,7,8</sup> In spite of this agreement, confirmation of these results by an independent method would be highly desirable. In addition, there are many questions into

which vibrational spectroscopy offers little insight: for instance, the bonding site of the hydroxyl groups, the occurrence of isolated or clustered water molecules, the spatial relationship between OH and  $\text{H}_2\text{O}$  species, and the motional state of  $\text{H}_2\text{O}$ .

Solid-state NMR spectroscopy is a powerful technique for the investigation of glassy systems since it provides selective information about the immediate environment of the nucleus being observed. Several proton NMR studies of water in glasses have appeared.<sup>9–12</sup> In the first detailed application of wideline NMR to this problem, Müller-Warmuth et al.<sup>9</sup> established a close proximity between protons and alkali metal cations in alkali silicate glasses by analyzing the compositional dependence of the second moment. Direct NMR evidence for the presence of molecular  $\text{H}_2\text{O}$  in addition to Si-OH groups was presented in a study by Bartholomew and Schreurs on hydrosilicate glasses.<sup>10</sup> The possibility of distinguishing between  $\text{H}_2\text{O}$  and OH groups in glasses by a mathematical analysis of the free induction decay was proposed,<sup>11</sup> and recently results on naturally occurring glasses with very low proton contents have been reported.<sup>12</sup>

Early wideline NMR studies of water in glasses utilized the line broadening arising from internuclear dipolar interactions as

<sup>†</sup> Caltech Division of Geological and Planetary Sciences contribution no. 4507.

<sup>‡</sup> Current address: Department of Chemistry, University of California at Santa Barbara, Goleta, CA 93106.

- (1) Bartholomew, R. F. *Treatise Mater. Sci. Technol.* **1982**, 22, 75.
- (2) Newman, S.; Epstein, S.; Stolper, E. M. *J. Volcanol. Geotherm. Res.*, in press.
- (3) Silver, L. A.; Stolper, E. M. submitted for publication in *J. Petrol.*
- (4) Tomozawa, M. *J. Non-Cryst. Solids* **1985**, 73, 197.
- (5) Burnham, C. W. *Geochim. Cosmochim. Acta* **1975**, 31, 1077.
- (6) Watson, E. B. *Earth Planet. Sci. Lett.* **1981**, 52, 291.
- (7) Stolper, E. M. *Contrib. Mineral. Petrol.* **1982**, 81, 1.
- (8) Stolper, E. M. *Geochim. Cosmochim. Acta* **1982**, 46, 209.
- (9) Müller-Warmuth, W.; Schulz, G. W.; Neuroth, N.; Meyer, F.; Deeg, N. Z. *Naturforsch. A: Astrophys., Phys., Phys. Chem.* **1965**, 20A, 902.
- (10) Bartholomew, R. F.; Schreurs, J. W. H. *J. Non-Cryst. Solids* **1980**, 38/39, 679.
- (11) Belton, P. S. *J. Chem. Technol. Biotechnol.* **1979**, 29, 19.
- (12) Bray, P. J.; Holupka, R. J. *Non-Cryst. Solids* **1984**, 67, 119.

TABLE I: Nominal Compositions of the Glass Systems under Study<sup>a</sup>

glass	SiO <sub>2</sub>	Al <sub>2</sub> O <sub>3</sub>	Na <sub>2</sub> O	K <sub>2</sub> O	CaO	FeO
A	68.74 (68.04)	19.44 (19.97)	11.82 (11.60)	(0.18)	(0.17)	(0.03)
O	64.76 (65.19)	18.32 (17.84)	(0.01)	16.92 (16.97)	(0.00)	(0.01)
AO	66.41 (67.77)	18.76 (18.11)	5.70 (5.65)	8.67 (8.42)	(0.00)	(0.01)
AO	65.64 (67.01)	18.55 (18.45)	5.64 (5.52)	8.57 (8.46)	(0.01)	1.04 (0.63)
AO	64.86 (66.68)	18.34 (18.38)	5.57 (5.30)	8.47 (8.21)	(0.01)	2.08 (1.41)
ASW	62.35 (63.02)	14.40 (13.92)	(0.33)	(0.02)	23.25 (22.66)	(0.03)
R	(77.50)	(12.50)	(3.90)	(4.80)	(0.53)	(1.00)

<sup>a</sup> Numbers in parentheses denote compositions determined by electron probe microanalysis. A = albite, O = orthoclase, AO = albite-orthoclase, ASW = anorthite-silica-wollastonite eutectic, R = rhyolite.

the major diagnostic tool. In contrast, recently developed high-resolution techniques increase the spectral resolution by removing these interactions and place emphasis upon the chemical shift as the major source of information. Although high-resolution conditions are especially difficult to achieve in proton NMR studies, where large homonuclear dipolar couplings predominate and chemical shift effects are small, the pioneering work of Haeberlen<sup>13</sup> and Vaughan and co-workers,<sup>14</sup> using multiple-pulse methods on single crystals, has provided a valuable data base of proton chemical shifts. A linear dependence of the isotropic chemical shift on the O—H...O bonding distance was noted for a wide range of crystalline compounds.<sup>14</sup> More accurate chemical shift measurements have been carried out using multiple-pulse methods in combination with MAS.<sup>15</sup> However, little work has been reported using high-speed <sup>1</sup>H MAS-NMR without multiple-pulse methods, a technique that preserves valuable information about homonuclear dipolar couplings.<sup>16</sup> Also, the application of high-resolution proton NMR to amorphous systems has, to date, been limited to a brief report on results obtained on dried silica gels.<sup>17</sup>

We present here the first systematic high-resolution <sup>1</sup>H MAS-NMR study of glassy systems. A major focus is the effect of the water content in a series of closely related synthetic and natural silicate glasses upon the hydrous species present. In addition to the structural information provided by NMR methods, the proportionality of the signal intensity to the number of contributing nuclei enables NMR to be used as a nondestructive means of determining absolute water contents and the concentrations of individual H-bearing species in glasses without paramagnetic ions. In the present study, we have addressed these quantitative aspects of <sup>1</sup>H wide-line and magic angle spinning NMR in detail and developed optimized conditions under which satisfactory results can be obtained both in naturally occurring and in synthetic samples.<sup>18</sup>

## Experimental Section

**Preparation of the Synthetic Glasses.** Samples with several different anhydrous glass compositions were studied: albite (A); orthoclase (O); albite-orthoclase (AO), with and without FeO; and the anorthite-silica-wollastonite eutectic (ASW). Table I

TABLE II: Synthesis Conditions and Water Contents of the Glasses under Study

glass	press., kbar	temp., °C	time, min	% H <sub>2</sub> O	
				manom	NMR
A	20	1400	140	0.96	1.05
	20	1400	140	1.04	0.99
	20	1400	140		2.22
	15	1225	120	2.97	2.97
	15	1100	120	4.76	4.60
	20	1400	140	5.59	5.82
	20	1450	90	0.96	1.01
	20	1400	05		1.50
	20	1450	90		1.87
	20	1450	90	1.93	1.92
O	20	1450	90	2.53	2.62
	15	1450	110		3.32
	20	1450	120	4.72	4.66
	15	1400	150		5.95
	20	1450	120		6.33
	20	1450	120	7.10	8.42
	15	1400	120	7.39	7.89
	20	1400	120	7.05	6.16 <sup>a</sup>
	20	1400	120	8.11	5.90 <sup>b</sup>
	20	1450	120	0.67	0.73
ASW	20	1450	120	0.99	1.06
	20	1450	120	1.76	1.73
	20	1450	120		6.96
	15	1400	120	7.93	7.87
	15	1400	120	8.82	8.76
				0.12	0.08
				0.41	0.27
				0.55	0.35
				0.69	0.45
				0.78	0.49
R <sup>c</sup>				1.52	0.90
				1.72	1.19
				2.02	1.33
				2.26	1.33
				2.56	1.65

<sup>a</sup> 0.58 wt % FeO. <sup>b</sup> 1.27 wt % FeO. <sup>c</sup> All rhyolites contain 0.96–1.04 wt % FeO.

lists the nominal compositions of these glass systems. Anhydrous AO glasses were prepared at Corning Glass Works from production grade oxides by melting at 1650 °C for 16 h. The other starting materials were crystalline Amelia albite (A) or mixtures of Johnson-Matthey SpecPure oxides (O, ASW), which were finely ground in ethanol, dried for 24 h at 800 °C, and stored over a desiccant. In the case of the albite and ASW glasses, the oxides were premelted at 1 atm and 1300 °C, quenched to glass, re-ground, and dried at 800 °C. The anhydrous starting materials or glasses together with a known amount of H<sub>2</sub>O were loaded into Pt capsules which were then sealed by arc welding. Capsules were run at 1400–1450 °C, 15–20 kbar in a 1.0-in. solid-media piston cylinder apparatus, containing a NaCl cell with a Pyrex sleeve and either boron nitride or fired pyrophyllite as the inner sleeve material, or in a 0.5-in. piston cylinder apparatus, using a talc cell with a Pyrex sleeve.<sup>3,19</sup> All of the samples were liquid under run conditions; they were quenched to glasses at ca. 150–200 °C/s by turning off the graphite furnace.

A sample of vitreous silica was prepared at Corning Glass by flame hydrolysis of SiCl<sub>4</sub> at 1000 °C and 1 atm and subsequent sintering. The water content of this sample was determined by infrared spectroscopy to be 0.04 wt %, using an extinction coefficient of 181 L/(mol·cm).<sup>20</sup>

**Origin of the Volcanic Glasses.** The volcanic glasses under study originate from the ca. 1340 A.D. eruption of the Mono Craters (Central California) and are of rhyolitic composition. They form a complete series of different water contents ranging from 0.1 to 2.6 wt % H<sub>2</sub>O, depending on their time sequence in the original eruption.<sup>2</sup> A volcanic glass sample containing several

(13) Haeberlen, U. *High Resolution NMR in Solids*; Academic: New York, San Francisco, London, 1976; p 149.

(14) Berglund, B.; Vaughan, R. W. *J. Chem. Phys.* **1980**, *73*, 2037 and references therein.

(15) Scheler, G.; Haubenreisser, U.; Rosenberger, H. *J. Magn. Reson.* **1981**, *44*, 134.

(16) Yesinowski, J. P.; Eckert, H. *J. Am. Chem. Soc.* **1987**, *109*, 6274.

(17) Rosenberger, H.; Scheler, G.; Bürger, H.; Jakob, M. *Colloids Surf.* **1984**, *12*, 53.

(18) Preliminary results have been presented: Eckert, H.; Yesinowski, J. P.; Stolper, E. M. *Eos, Transactions of the American Geophysical Union* **1985**, *66*, 1139. Yesinowski, J. P.; Eckert, H. Poster presented at the 26th Experimental NMR Conference, Baltimore, MD, 1986.

(19) Fine, G.; Stolper, E. M. *Contrib. Mineral. Petrol.* **1985**, *91*, 105.

(20) Shelby, J. E.; Vitko, J., Jr.; Benner, R. E. *J. Am. Ceram. Soc.* **1982**, *65*, C59.

weight percent water isotopically diluted with  $D_2O$  was made by hydration of Los Posos rhyolite with  $(H_{0.10-0.15}D_{0.90-0.85})_2O$  at 700 bar and 850 °C for several days in a rapid quench vessel.<sup>21</sup>

**Analytical Characterization of the Glass Samples.** Selected samples of each glass composition were analyzed with an automated JEOL 733 Superprobe electron microprobe to verify glass composition and homogeneity, to assess possible Na and K loss during the synthesis of the anhydrous starting materials, and to determine Fe contents. These analyses were carried out with a 15-kV accelerating voltage, a sample current of 5 nA, and a 20–25  $\mu m$  spot size. These data, reported in Table II, represent the averages of 5–10 measurements on different sampling points. Total water contents were determined by a manometric technique described earlier,<sup>22</sup> and infrared spectra were obtained on ca. 5–10 doubly polished thin sections of each glass sample by using a Nicolet 60SX FTIR spectrometer. The details and results of the infrared spectroscopic work will be reported elsewhere.<sup>3,23</sup> Synthesis conditions and analytical data for the glasses under study are listed in Table II. *The concentrations of both OH and  $H_2O$  species are reported as the amount of water that would be released on heating if all species were released as  $H_2O$ .*

Reference NMR data were obtained on powdered samples prepared from single crystals of the minerals tremolite,  $Ca_2Mg_5Si_8O_{22}(OH)_2$ ; pyrophyllite,  $Al_2Si_4O_{10}(OH)_2$ ; analcite,  $NaAlSi_2O_6 \cdot H_2O$ ; and gypsum,  $CaSO_4 \cdot 2H_2O$ . The water content of the pyrophyllite sample (from Mariposa Co., CA) used for absolute quantitation purposes was determined to be  $4.98 \pm 0.06$  wt % by manometry.<sup>22</sup> The tremolite and analcite samples used in fitting the MAS-NMR spectra of the hydrous glasses were high-quality single-crystalline materials from the mineral collection of the California Institute of Technology. Electron microprobe analysis confirmed that the tremolite sample was close to the theoretical stoichiometry and contained very little iron (0.1 wt %). The identity of the analcite sample was confirmed by X-ray powder diffraction.

**NMR Experiments.** Room temperature nuclear magnetic resonance spectra were recorded at 200.27 MHz on a homebuilt spectrometer system interfaced with a Nicolet 293B pulse programmer, Explorer fast digitizer, and Nicolet 1280 computer system. Details of the spectrometer have been described elsewhere.<sup>21</sup> Wideline NMR spectra were obtained on 100–300-mg samples of coarsely ground powders ( $>44$ – $300 \mu m$ ) or glass chunks in a homebuilt probe with a 5 mm diameter solenoidal coil. A solid echo pulse sequence<sup>24</sup> ( $90^\circ_x - \tau - 90^\circ_y - \tau$ -acquire) was used to circumvent the spectrometer "dead time" after an rf pulse. The  $90^\circ$  pulse length was 1.8–2  $\mu s$ ; typically, a refocusing delay  $\tau$  of 8  $\mu s$  was used. Spin-lattice relaxation times were measured by using the inversion recovery sequence. The recycle delay times were always chosen to be at least 5 times as long as the experimentally measured spin-lattice relaxation times  $T_1$ , which were found to be ca. 0.05 and 1–10 s in the volcanic and the synthetic glass samples, respectively. (No systematic trends of  $T_1$  with glass composition or absolute water content were observed.) Typically, 64 scans were acquired and processed with an exponential line-broadening function of 100 Hz.

$^1H$  magic angle spinning spectra were obtained at 200.27 MHz and at 500.13 MHz (the latter using a Bruker WM-500 spectrometer). Finely ground powders (44–150  $\mu m$ ) were packed into 5 mm o.d. sapphire rotors which were spun in high-speed magic angle spinning probes from Doty Scientific. Both probes were specially designed to yield as low a proton background as possible. At 200 MHz, spectra were acquired with  $45^\circ$  pulses (1.0  $\mu s$ ); 10– $30^\circ$  pulses were used at 500.13 MHz in order to improve the uniformity of excitation across the spectrum, due to the lower pulse power available ( $90^\circ$  pulse length at 500 MHz = 8  $\mu s$ ). For each sample, spectra were obtained at a series of different spinning

speeds, ranging from 2.0 to 8.0 kHz. Typically, 64 free induction decays were acquired and then processed with an exponential line-broadening function of 50 Hz. Chemical shifts were determined by using the hydroxyl resonance of a hydroxyapatite sample ( $\delta_{iso} = 0.2$  ppm with respect to TMS) as a secondary reference.<sup>16</sup>

## Results

Figure 1 shows typical  $^1H$  wideline NMR spectra of some synthetic orthoclase and albite glasses. These spectra are characteristic of solid-state NMR powder patterns, and show that the hydrogen-bearing species do not exhibit isotropic mobility at room temperature. Thus, water is present not in the form of liquidlike "pools" or inclusions in any detectable amounts, but rather in forms such as anisotropically constrained OH and  $H_2O$  species.

In this section, we describe the NMR methodology used in the present study to measure absolute  $H_2O$  contents and determine the concentrations of distinguishable H-bearing species (i.e.,  $H_2O$  and OH) in these synthetic glass systems. The extension of these analytical approaches to the study of naturally occurring glasses, and the structural inferences to be drawn from the MAS-NMR spectra, will be discussed in the next section.

**Methodology of  $H_2O$  Quantitation.** The direct proportionality of the area under an NMR peak to the number of nuclear spins contributing to that peak is the basis of quantitative NMR applications. As detailed below, this approach to measuring the water content of glasses by wideline NMR encounters several complications. The finite spectrometer dead time necessitates a certain delay (ca. 10  $\mu s$  in the present study) before useful data acquisition can begin after a pulse. A substantial irreversible magnetization decay occurs during this dead time for the present samples, resulting in signal loss and line-shape distortions. The solid echo pulse sequence circumvents the dead-time problem by refocusing the homonuclear dipolar couplings to produce an echo signal some time  $\tau$  after the second pulse. However, the refocusing effect strictly applies only to an isolated pair of spins with  $I = 1/2$ .<sup>24</sup> In the presence of multiple homonuclear dipolar interactions, an irreversible magnetization decay (with a time constant  $T_2^*$ ) occurs during the evolution period  $\tau$ , resulting in an incomplete echo formation. Thus, serious quantitation errors can be introduced if the  $T_2^*$  values differ greatly among the samples studied and the standards used. To address this question, we monitored this magnetization decay by measuring the integrated signal intensity as a function of  $\tau$  for different glass samples and several crystalline model compounds (tremolite,  $Ca_2Mg_5Si_8O_{22}(OH)_2$ , and pyrophyllite,  $Al_2Si_4O_{10}(OH)_2$ , for OH groups; gypsum,  $CaSO_4 \cdot 2H_2O$ , and analcite,  $NaAlSi_2O_6 \cdot H_2O$ , for  $H_2O$  groups). Figure 2 shows a representative decay curve observed for an orthoclase glass containing 2.6 wt %  $H_2O$ . For all of the glasses investigated, one can obtain an approximate  $T_2^*$  decay constant by fitting the data for  $8 \mu s < \tau < 100 \mu s$  to a single-exponential decay. The estimates of  $T_2^*$  thus obtained are listed in Table III. (No obvious dependence of these  $T_2^*$  values on the basic glass composition or the absolute water content could be found.) The  $T_2^*$  decay curve of pyrophyllite was found to be very similar to those of the glasses, yielding a much better agreement with the latter than any of the decay curves observed for the other crystalline reference compounds. Hence, pyrophyllite was used as the standard for all of the glasses studied. The water contents measured by this NMR method (accuracy ca.  $\pm 5\%$ ) are listed in Table II and compared in Figure 3 to analytical data obtained by manometry.

**Methodology of Determining  $H_2O$  and OH Species Concentrations.** In addition to the total water content, the relative amounts of hydroxyl groups and molecular water groups are also of interest. It is clearly seen in Figure 1 that the spectra of all of the glasses contain two distinct components: a broad line suggestive of the "Pake doublet"<sup>25</sup> observed for molecular water units in crystalline hydrates such as analcite and gypsum, and a sharper component that has been assigned to hydroxyl groups.<sup>9,10</sup> Figure 1 shows that, with increasing  $H_2O$  content, the signal contribution due to the broader component increases, reflecting

(21) Eckert, H.; Yesinowski, J. P.; Stolper, E. M.; Stanton, T. R.; Hollaway, J. R. *J. Non-Cryst. Solids* **1987**, *93*, 93.

(22) Newman, S.; Stolper, E. M.; Epstein, S. *Am. Mineral.* **1986**, *71*, 1527.

(23) Silver, L. A.; Ihinger, P. D.; Stolper, E. M., to be submitted for publication.

(24) Powles, J. G.; Strange, J. H. *Proc. Phys. Soc., London* **1963**, *82*, 6.

(25) Pake, G. E. *J. Chem. Phys.* **1948**, *16*, 327.

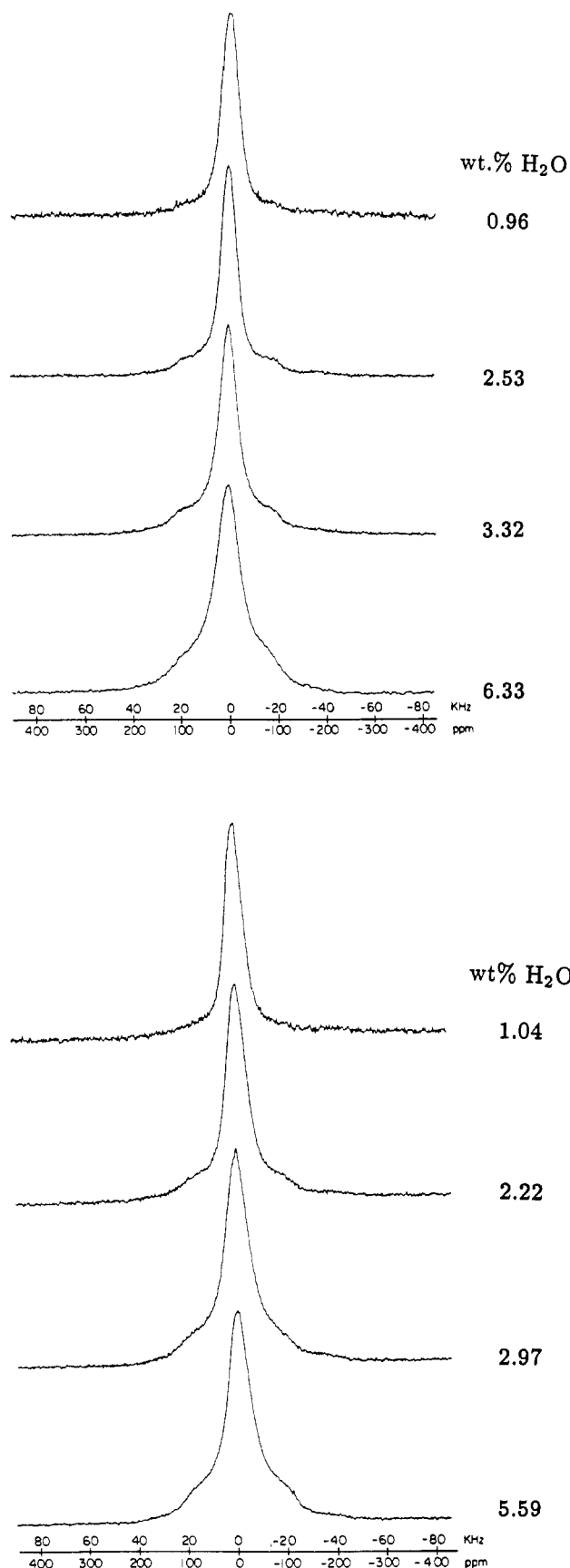


**Figure 1.** (a, top) Solid echo  $^1\text{H}$  NMR spectra at 200.27 MHz of orthoclase glasses with different water contents determined by  $\text{H}_2$  manometry. Refocusing delay 8  $\mu\text{s}$ , recycle delay 60 s, 64 scans; Lorentzian line broadening 100 Hz. (b, bottom) Solid echo  $^1\text{H}$  NMR spectra at 200.27 MHz of albite glasses with different water contents determined by  $\text{H}_2$  manometry. Refocusing delay 8  $\mu\text{s}$ , 64 scans, recycle delay 60 s; Lorentzian line broadening 100 Hz.

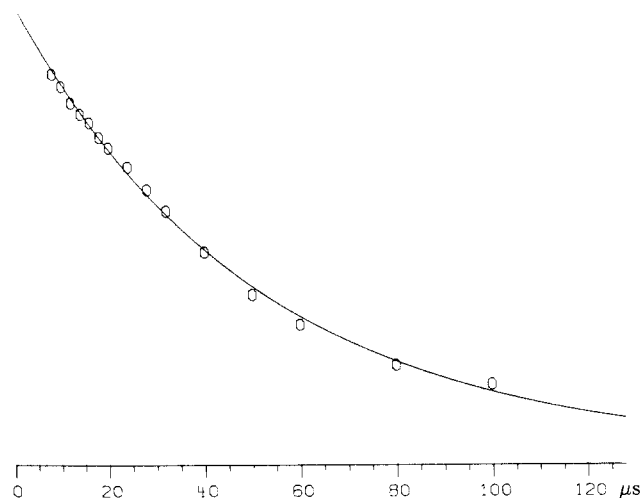


**Figure 2.**  $T_2^*$  decay curve ( $^1\text{H}$  NMR at 200.27 MHz) of an orthoclase glass containing 2.6 wt %  $\text{H}_2\text{O}$ , recycle delay 60 s. The ordinate is the integrated area (arbitrary linear units) of the Fourier-transformed echo signal; the abscissa is the refocusing delay of the solid-echo pulse sequence. The data are fitted by a Lorentzian decay curve with  $T_2^* = 50.4 \pm 0.5 \mu\text{s}$ .

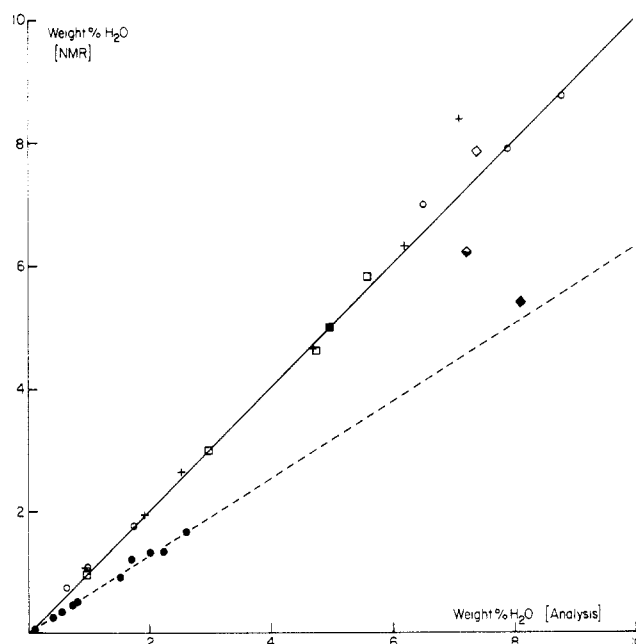


**Figure 3.** Water content determined by solid echo  $^1\text{H}$  NMR at 200.27 MHz versus water content determined by manometric analysis (see text). The solid line represents the identity. The dashed line is a guide to the eye for the natural rhyolitic glasses. albite composition,  $\square$ ; orthoclase composition,  $+$ ; albite-orthoclase composition, 0.01 wt %  $\text{FeO}$  ( $\diamond$ ), 0.58 wt %  $\text{FeO}$  ( $\blacklozenge$ ), 1.27 wt %  $\text{FeO}$  ( $\blacklozenge$ ); ASW composition,  $\circ$ ; volcanic rhyolite glasses,  $\bullet$ ; pyrophyllite (standard),  $\blacksquare$ .

an increasing fraction of molecular  $\text{H}_2\text{O}$  species.

Earlier results by Bartholomew and Schreurs<sup>10</sup> indicated that it might be possible to analyze these trends in some fashion to obtain the respective OH and  $\text{H}_2\text{O}$  contents of these glasses. Such a quantitative line-shape decomposition is, however, very difficult in practice, since the individual line shapes of these species are unknown and difficult to predict because of the additional broadening effects often observed in glasses arising from distributions of isotropic and anisotropic chemical shifts. Also, discrimination of both spectral components on the basis of different spin-lattice relaxation times (used in a previous  $^2\text{H}$  NMR study of water in glasses<sup>21</sup>) is rendered impossible by fast spin diffusion.

Figure 4 shows that high-speed magic angle spinning dramatically improves the resolution of the  $^1\text{H}$  spectra of glasses. The spectra consist of a relatively sharp, intense center band at the

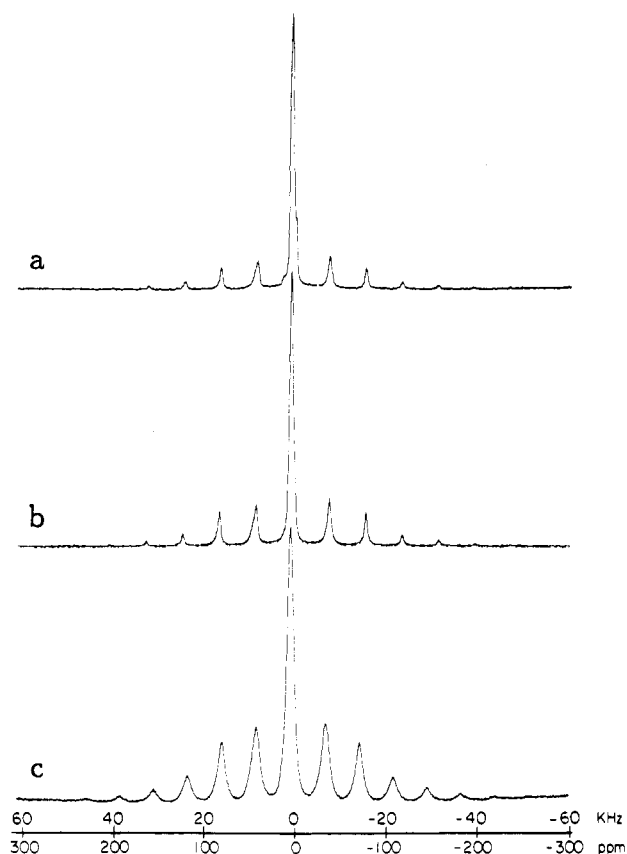


**Figure 4.**  $^1\text{H}$  MAS-NMR spectra at 200.27 MHz of water-containing glasses. Spinning speed 8.0 kHz.  $45^\circ$  pulse, recycle delay 10 s, 64 scans, line broadening 50 Hz. (a) Orthoclase glass containing 1.50 wt %  $\text{H}_2\text{O}$ . (b) Orthoclase glass containing 2.53 wt %  $\text{H}_2\text{O}$ . (c) Anorthite-silica-wollastonite glass containing 7.93 wt %  $\text{H}_2\text{O}$ .

isotropic chemical shift position and a set of associated spinning side bands spaced at integer multiples of the spinning speed  $\nu_r$ . At a constant resonance frequency (200.27 MHz) and spinning speed (8.0 kHz) increased relative intensity is distributed into the spinning sidebands as the total water content of the glasses is increased. In the following, we outline how this effect can be used to obtain the percentages of OH and molecular  $\text{H}_2\text{O}$  can be obtained.

As theoretically predicted<sup>26</sup> and experimentally observed,<sup>16,27</sup> the sideband intensity patterns observed in  $^1\text{H}$  MAS-NMR spectra are significantly different for OH and  $\text{H}_2\text{O}$  groups in crystalline compounds. For rigid OH groups the spinning sideband intensities are governed by the  $^1\text{H}$  chemical shift anisotropy as well as homonuclear and heteronuclear dipole-dipole interactions (e.g., with  $^{23}\text{Na}$  and  $^{27}\text{Al}$ ). Under the experimental conditions used, the hydroxyl groups exhibit only one or two pairs of spinning sidebands with rapidly diminishing intensities. For example, the 200.27-MHz  $^1\text{H}$  MAS-NMR spectrum (Figure 5, top) of the structurally isolated OH groups in the mineral tremolite demonstrates that the dominant contribution to the spectral area (86% at  $\nu_r = 8$  kHz) arises from the centerband.

In contrast, structural  $\text{H}_2\text{O}$  in crystal hydrates gives rise to much wider spinning sideband patterns, extending over ca. 100 kHz. This characteristic intensity pattern, the envelope of which resembles that of a Pake doublet in the slow-spinning limit, arises mainly from the strong homonuclear dipole-dipole interaction, which is inhomogeneous in character for an isolated pair of nuclear spins.<sup>26</sup> As an example, Figure 5 (bottom) shows the  $^1\text{H}$  MAS-NMR spectrum of analcite, a compound with structurally isolated  $\text{H}_2\text{O}$  groups. Only a minor fraction of the total signal area (18%) is contained in the MAS centerband.

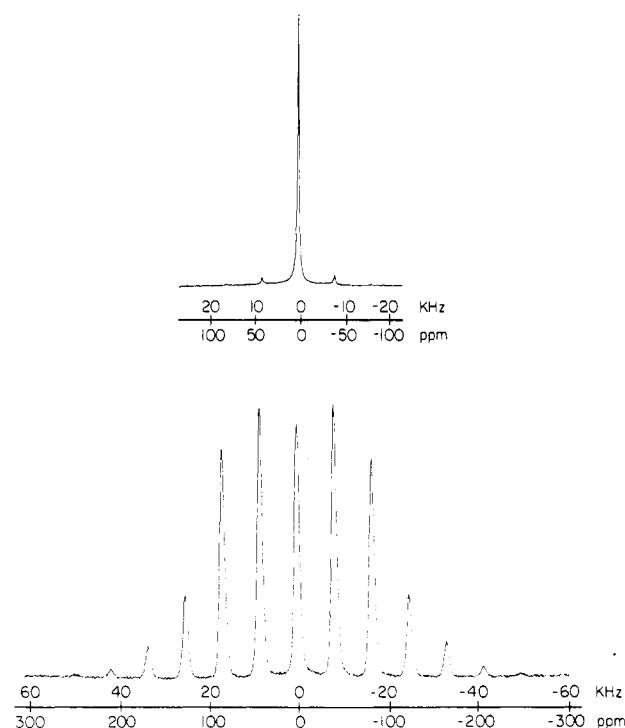


**Figure 5.**  $^1\text{H}$  MAS-NMR spectra at 200.27 MHz of model compounds. Spinning speed 8.0 kHz.  $45^\circ$  pulse, recycle delay 10 s, 32 scans; line broadening 50 Hz. (top) Tremolite,  $\text{Ca}_2\text{Mg}_5\text{Si}_8\text{O}_{22}(\text{OH})_2$ ; (bottom) Analcite,  $\text{NaAlSi}_2\text{O}_6 \cdot \text{H}_2\text{O}$ .

The substantial differences between the spinning sideband patterns observed for the model compounds tremolite (OH) and analcite ( $\text{H}_2\text{O}$ ) suggest that in samples containing both  $\text{H}_2\text{O}$  and OH, the intensity profile of the spinning sideband pattern could serve as a measure of their relative percentages. The simplest approach is to consider the spectrum of the glasses as the sum of the weighted individual MAS-NMR peak patterns of OH and  $\text{H}_2\text{O}$  in the model compounds, ignoring the small chemical shift difference, and assuming that these peak patterns are not modified by dipolar interactions between these species.

To test the validity of the latter assumption, we compared the MAS-NMR center- and sideband intensities (as measured by peak heights) observed in the synthetic glasses with those obtained by adding properly weighted individual spectra of tremolite and analcite. Best-fit simulated spectra were obtained by constraining both the centerband peak heights as well as the sums of the centerband and all sideband intensities to be equal for experimental and simulated spectra. The percentages of water present as molecular  $\text{H}_2\text{O}$  based on this procedure at a spinning speed of 8 kHz are listed in Table III. Figures 6a-c compare these simulations with the experimental spectra (the constrained centerbands are omitted). The agreement between experimental and simulated sideband intensities, especially at the highest spinning speed (8 kHz), supports the hypothesis that, at such speeds, the OH and  $\text{H}_2\text{O}$  species in these glasses can be treated as noninteracting species. While at 8 kHz the impact of the dipolar interactions between OH and  $\text{H}_2\text{O}$  species on the spinning sideband patterns is inferred to be minimal, more pronounced differences between experimental and simulated spectra occur at lower spinning speeds. This is especially apparent for the first spinning side-band pair at 5 kHz, shown in Figure 6c. Thus, the highest possible spinning speeds ( $>8$  kHz) are desirable in this analysis.

Since the line widths of the sidebands may differ among each other and from that of the centerband for several reasons, it is generally preferable to use integrated areas rather than peak heights for quantitative studies. Consequently, we developed an alternate procedure for determining the  $\text{H}_2\text{O}$  and OH percentages by using the area ratio

$$P = \frac{\text{area}(\text{centerband})}{\text{area}(\text{centerband} + \text{sidebands})}$$

(26) Maricq, M. M.; Waugh, J. S. *J. Chem. Phys.* **1979**, *70*, 3300.

(27) Yesinowski, J. P.; Eckert, H.; Rossman, G. R. *J. Am. Chem. Soc.*, in press.

TABLE III: 200.27-MHz  $^1\text{H}$  NMR Results for Glasses and Model Compounds Studied by Solid Echo and MAS-NMR<sup>a</sup>

sample	total water content, <sup>b</sup> % $\text{H}_2\text{O}$	$T_2^*$ , $\mu\text{s}$	$\delta_{\text{iso}}$ , ppm ( $\pm 0.2$ ppm)	$\Delta\nu_{1/2}$ , Hz ( $\pm 20$ Hz)	$\Delta d(\text{O}-\text{H}\cdots\text{O})$ , pm	ratio $\text{H}_2\text{O}/\text{OH}$		
						NMR sideband intensities	NMR integrn	IR
$\text{SiO}_2$	ca. 0.04		3.2	250	$\pm 2.5$	0/100	0/100	0/100
A	2.22 <sup>c</sup>		4.8	950	$\pm 9.3$	37.1/62.9	40.4/59.6	33.8/66.2
	2.97	$52.0 \pm 0.6$						
	4.76	$42.0 \pm 0.8$	5.1	1280 <sup>d</sup>	$\pm 12.6^d$		57.1/42.9 <sup>d</sup>	55.6/44.4
	5.59 <sup>e</sup>	$39.9 \pm 0.5$	5.3	1140	$\pm 11.2$	46.1/53.9	54.9/45.1	61.5/38.5
O	0.96	$43.1 \pm 0.4$	4.8	900 <sup>d</sup>	$\pm 8.8^d$		23.1/76.9 <sup>d</sup>	20.0/80.0
	1.50 <sup>c</sup>		4.6	840	$\pm 8.2$	34.3/65.7	32.8/67.2	30.0/70.0
	1.87 <sup>c</sup>		4.7	900	$\pm 8.8$	322.4/67.6	36.7/63.3	35.3/64.7
	1.96		4.7	920	$\pm 9.0$	32.9/67.1	41.2/58.8	35.8/64.2
	2.53	$50.4 \pm 0.5$	4.7	920	$\pm 9.0$	45.0/55.0	48.1/51.9	42.6/57.4
	3.32 <sup>c</sup>	$55.1 \pm 0.6$	5.1	1100	$\pm 10.8$	45.3/54.7	48.4/51.6	51.2/48.8
	5.95 <sup>c,e</sup>	$44.3 \pm 0.6$	4.8	1200	$\pm 11.8$	46.1/53.9	54.1/45.9	67.2/32.8
AO	7.39	$35.6 \pm 0.3$	5.0	1630 <sup>f</sup>	$\pm 16.0^f$	56.7/43.3	59.1/40.9	71.9/28.1
	8.11	$22.4 \pm 0.3$	5.6	2200	<sup>g</sup>	<sup>g</sup>	<sup>g</sup>	
ASW	0.99		5.2	1050 <sup>d</sup>	$\pm 10.3^d$		18.9/81.1 <sup>d</sup>	11.7/88.3
	7.93	$32.5 \pm 0.3$	4.8	1660	$\pm 16.3$	63.5/36.5	67.3/32.7	69.6/30.4
	8.82	$40.1 \pm 0.9$						
R	0.69	$49.0 \pm 2.0$	4.3	1610	<sup>g</sup>	<sup>g</sup>	<sup>g</sup>	
	0.78		4.2	1410	<sup>g</sup>	<sup>g</sup>	<sup>g</sup>	
	1.25		4.3	1680	<sup>g</sup>	<sup>g</sup>	<sup>g</sup>	
	2.26	$36.8 \pm 1.0$	4.3	1550	<sup>g</sup>	<sup>g</sup>	<sup>g</sup>	
pyrophyllite	4.98	$46.8 \pm 0.6$	2.3	850	<sup>f</sup>			
tremolite		$53.8 \pm 1.8$	0.7	320	<sup>f</sup>			
analcite		$46.2 \pm 1.3$	3.1	1270	<sup>f</sup>			
gypsum		$21.7 \pm 0.2$	5.3	3200	<sup>f</sup>			

<sup>a</sup>  $T_2^*$  is the decay time of the solid echo,  $\delta_{\text{iso}}$  is the chemical shift with respect to TMS determined by MAS-NMR,  $\Delta\nu_{1/2}$  is the full width at half-height of the MAS-NMR centerband, which was used to calculate  $\Delta d(\text{O}-\text{H}\cdots\text{O})$ , the distribution of  $\text{O}-\text{H}\cdots\text{O}$  distances about the mean value (see text).  $\text{H}_2\text{O}/\text{OH}$  ratios determined by infrared spectroscopy and two MAS-NMR procedures are given in terms of weight percent  $\text{H}_2\text{O}$  for both species (see text). A = albite, O = orthoclase, AO = albite-orthoclase, ASW = anorthite-silica-wollastonite eutectic, R = (volcanic) rhyolite. <sup>b</sup> By  $\text{H}_2$  manometry, error  $\pm 3\%$ . <sup>c</sup> By NMR, error  $\pm 5\%$ . <sup>d</sup> Determined at spinning speeds less than 5 kHz. <sup>e</sup> Samples with inhomogeneous distribution of water. <sup>f</sup> Line width partly determined by homonuclear dipole couplings, from field-dependence studies. <sup>g</sup> Determination precluded by effects of paramagnetic Fe(II) and Fe(III).

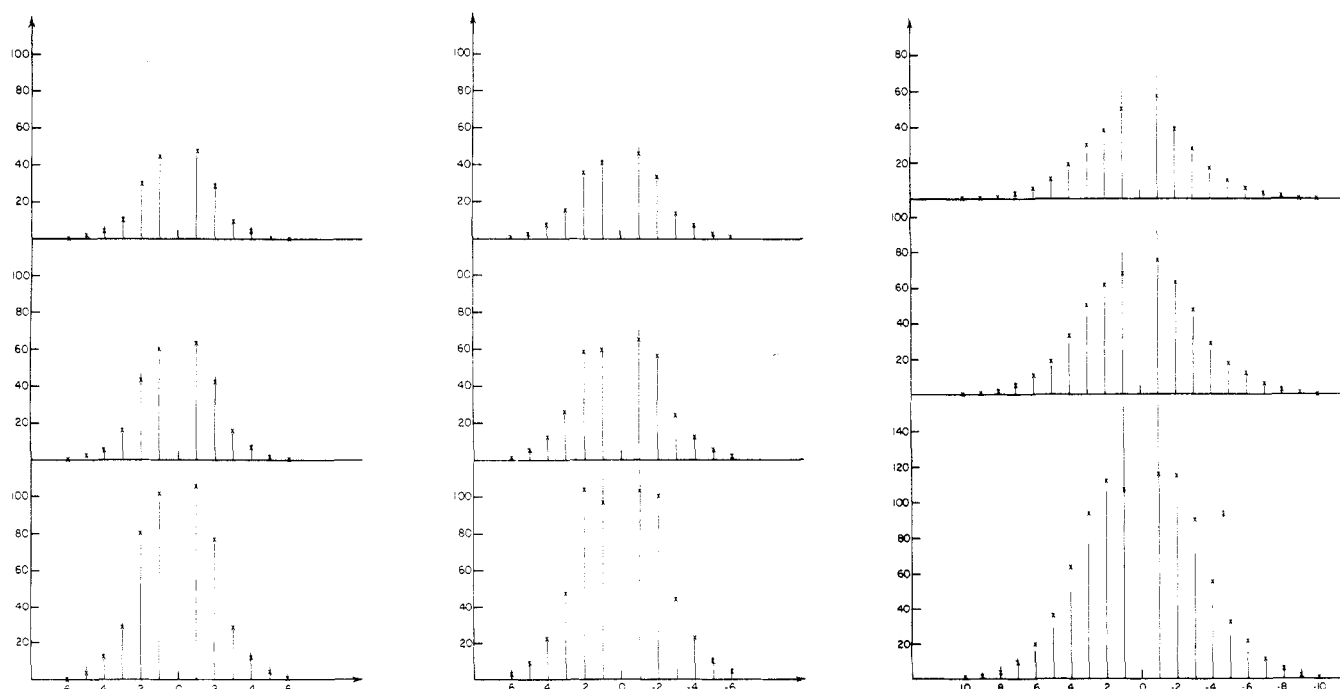
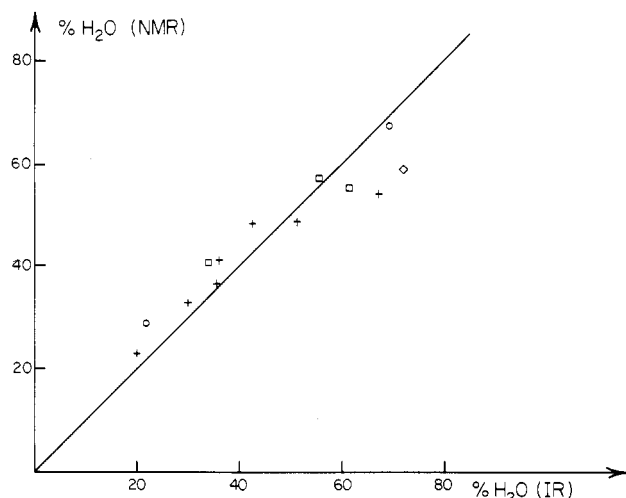


Figure 6.  $^1\text{H}$  MAS-NMR (200.27 MHz) spinning sideband peak heights (in arbitrary intensity units) for the three glasses of Figure 4. Solid lines represent experimental results, crosses are heights predicted by additive superposition of the experimental spectra of analcite and tremolite. The centerbands (not shown) have been scaled to identical heights for all figures. (a, left) Spinning speed 8.0 kHz. (b, center) Spinning speed 7.0 kHz. (c, right) Spinning speed 5.0 kHz.

At a spinning speed of 8 kHz,  $P = 0.855$  for tremolite (100% OH) and  $P = 0.183$  for analcite (100%  $\text{H}_2\text{O}$ ). Linear interpolation between these values yields the percentages of water present as OH and  $\text{H}_2\text{O}$  from the values for  $P$  measured for the glasses. Following this procedure, we found the results to be independent of the spinning speed above 6 kHz. Below this limit, the  $\text{H}_2\text{O}/\text{OH}$

ratios obtained from this analysis tend to increase, presumably reflecting a breakdown of the assumption that OH and  $\text{H}_2\text{O}$  are noninteracting species. Table III lists the results of this procedure and shows that the percentages of water present as molecular  $\text{H}_2\text{O}$  species obtained by the two different methods discussed above are generally in good agreement.



**Figure 7.** Percentage of water present as molecular  $\text{H}_2\text{O}$  determined by analyzing the fractional  $^1\text{H}$  MAS-NMR (200.27 MHz) centerband area versus percentage of water present as molecular  $\text{H}_2\text{O}$  determined by infrared methods (see text). Symbols as in Figure 3.

## Discussion

**Quantitative Analysis by  $^1\text{H}$  Wideline NMR.** The hydrogen contents of the synthetic iron-free glasses obtained from the  $^1\text{H}$  solid echo NMR quantitation agree very well with those obtained by hydrogen manometry (Figure 3). In contrast, for volcanic glasses the NMR quantitation values are only ca. 70% of the manometric values. We attribute the signal loss observed in the volcanic glasses to the presence of paramagnetic constituents (all volcanic glass samples contain ca. 1 wt % FeO, see Table II), because we observe similar effects in iron-containing synthetic glasses. Thus, in two albite/orthoclase samples containing ca. 8 wt %  $\text{H}_2\text{O}$  and 0.58 and 1.27 wt % FeO, respectively, the observable fractions of water were determined to be 87.4% and 73.2%, respectively. These results show that the loss of signal intensity is roughly proportional to the level of iron in the glass. The linearity of the NMR quantitation in Figure 3 for all of the volcanic glasses studied indicates that the scaling factors are essentially identical, consistent with microprobe analyses, which indicate that variations in iron contents among these glasses are small. The present results suggest that NMR can be calibrated to obtain absolute water contents in naturally occurring as well as synthetic glasses if the concentration of paramagnetic constituents is known.

The experimentally observed signal loss in Fe-bearing glasses is attributed to extreme broadening caused by the strong dipolar interactions between the hydrogen nuclei and nearby unpaired electron spins on the paramagnetic ion. The NMR results show that neither water molecules nor OH groups are associated preferentially with the iron ions, since such behavior would not lead to the dependence observed in Figure 3 (i.e., a straight line through the origin).

Our results demonstrate that  $^1\text{H}$  NMR is a quantitative, nondestructive method for determining water contents in glasses that requires virtually no sample preparation. Based on the favorable sensitivity of high-field proton NMR, quantitation at levels as low as 0.001 wt %  $\text{H}_2\text{O}$  should be possible. Because the background signal from the probe itself dominates at such low concentrations, we estimate that in the present study the lowest water content measurable with reliable accuracy ( $\pm 5\%$ ) was ca. 0.05 wt % in a 200-mg sample.

**$^1\text{H}$  MAS-NMR Determination of  $\text{H}_2\text{O}$  and OH Species Concentrations.** Figure 7 compares determinations of the speciation of water in glasses obtained from  $^1\text{H}$  MAS-NMR integrations of center- and sidebands with results obtained from infrared spectroscopy. The percentage of water occurring in the form of molecular  $\text{H}_2\text{O}$  determined by NMR is plotted against the corresponding values from IR results. The agreement between these independent methods is very good. One advantage of the

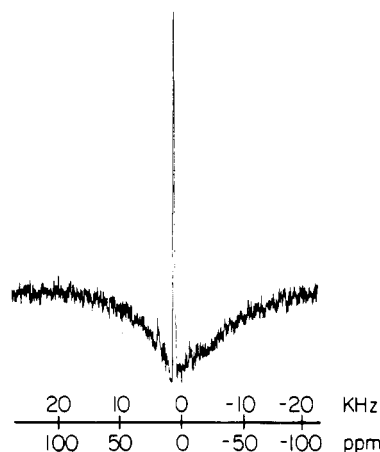


**Figure 8.** The 200.27-MHz  $^1\text{H}$  MAS-NMR spectrum of vitreous silica containing 0.04 wt %  $\text{H}_2\text{O}$ . Inversion recovery experiments were used to separate the signal of the sample from probe background absorption. The negative excursion in the base line arises from the probe background, which remains unaffected by the inversion recovery sequence. Recycle delay 600 s, 32 scans. Spinning speed 3.3 kHz.

MAS-NMR speciation is its generality. While determination of the speciation of water in glasses by infrared spectroscopy requires that the extinction coefficients for OH and  $\text{H}_2\text{O}$  species be determined by laborious calibration experiments,<sup>3,22,23</sup> the NMR analysis can be performed on any glass as long as the level of paramagnetic constituents is low. On the other hand, the MAS-NMR speciation procedure requires more material and is model dependent; it assumes that the ratio of the centerband area to the total signal area in tremolite is the same as that of the OH species in the glasses, and that the corresponding ratio in analcite is identical with that of the  $\text{H}_2\text{O}$  species in the glasses. The good agreement between the calculated and experimental spinning sideband intensities (especially Figure 6a), the weak dependence of the results upon spinning speeds (between 5 and 8 kHz), as well as the compatibility of these analyses with the infrared results indicate that this assumption is justified at sufficiently high spinning speeds. Further support is provided by the  $^1\text{H}$  MAS-NMR spectrum (Figure 8) of a vitreous silica sample containing ca. 0.04 wt % water, which is known from infrared spectroscopy to contain only OH groups. Even at a significantly lower spinning speed (3.3 kHz), the spinning sidebands in this silicate glass are extremely weak and hardly detectable above the noise level. This is similar to the observed weak spinning sidebands in the spectrum of tremolite. The suitability of tremolite and analcite to represent OH and  $\text{H}_2\text{O}$  groups in glasses leads to interesting conclusions concerning the proximity of the hydrous species, as discussed in the next section.

For glasses containing significant levels of paramagnetic ions, the MAS-NMR sideband pattern analysis described in the Results section cannot be used to obtain the percentages of  $\text{H}_2\text{O}$  and OH species. Figure 9a shows  $^1\text{H}$  MAS-NMR spectra for two albite-orthoclase glasses containing zero and 1.27 wt % FeO and comparable levels of  $\text{H}_2\text{O}$ . This comparison illustrates that the presence of paramagnetic iron in glasses results in more intense spinning sidebands. This sideband enhancement is also seen in the volcanic glasses of the present study (data not shown), where the experimentally observed spinning sideband intensities are much higher than expected from the spectra observed for synthetic glasses with similar water contents. A similar effect has been noted by Murdoch et al. in the  $^{29}\text{Si}$  NMR spectra of albitic glasses.<sup>28</sup> The origin of this behavior lies with the dipolar interactions between protons and unpaired electron spins, which affect the  $^1\text{H}$  NMR line shapes, as illustrated in spectra of nonspinning samples (Figure 9b,c). The signals reveal a characteristically broadened "tent shape" in which the distinction between OH and  $\text{H}_2\text{O}$  signal components is gradually lost. Theoretical calculations reveal that

(28) Murdoch, J. B.; Stebbins, J. F.; Carmichael, I. S. E. *Am. Mineral.* 1985, 70, 332.



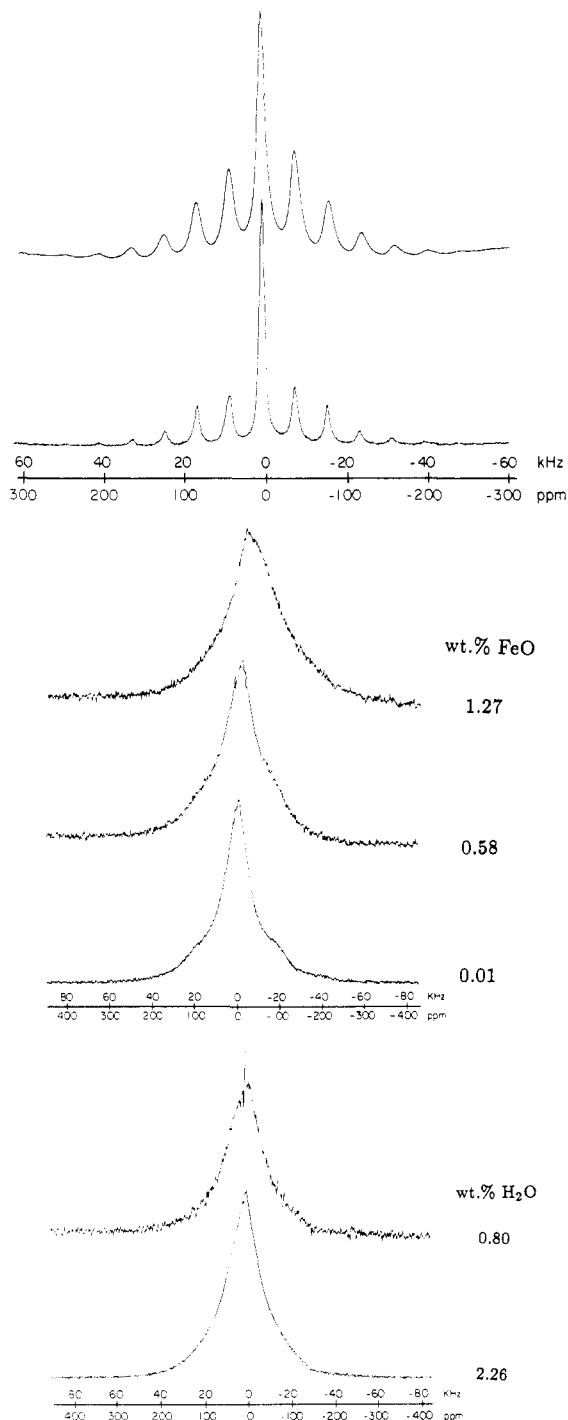


**Figure 9.** Influence of iron content upon the 200.27 MHz  $^1\text{H}$  NMR spectra of water-containing glasses (a, top)  $^1\text{H}$  MAS-NMR spectra of synthetic albite-orthoclase glasses,  $45^\circ$  pulse, recycle delay 10 s (5 s for iron-containing glass), 64 scans: (upper) 8.10 wt %  $\text{H}_2\text{O}$ , 1.27 wt % FeO; (lower) 7.39 wt %  $\text{H}_2\text{O}$ , 0.01 wt % FeO. (b, middle)  $^1\text{H}$  solid echo NMR spectra of synthetic albite-orthoclase glasses.  $90^\circ$  pulse length 1.9  $\mu\text{s}$ , refocusing delay 8  $\mu\text{s}$ , recycle delay 60 s, 64 scans, line broadening 50 Hz. From top to bottom: 8.10 wt %  $\text{H}_2\text{O}$ , 1.27 wt % FeO; 7.05 wt %  $\text{H}_2\text{O}$ , 0.58 wt % FeO; 7.39 wt %  $\text{H}_2\text{O}$ , 0.01 wt % FeO. (c, bottom)  $^1\text{H}$  solid echo NMR spectra of volcanic rhyolite glasses.  $90^\circ$  pulse length 2.0  $\mu\text{s}$ , refocusing delay 8  $\mu\text{s}$ , recycle delay 1 s, 64 scans.

these dipolar interactions, which are inhomogeneous in character, contribute substantially to MAS-NMR spinning sideband intensities.<sup>29</sup>

**Spatial Relationships between OH and  $\text{H}_2\text{O}$  Species.** At high spinning speeds the experimental  $^1\text{H}$  MAS-NMR spectra of the

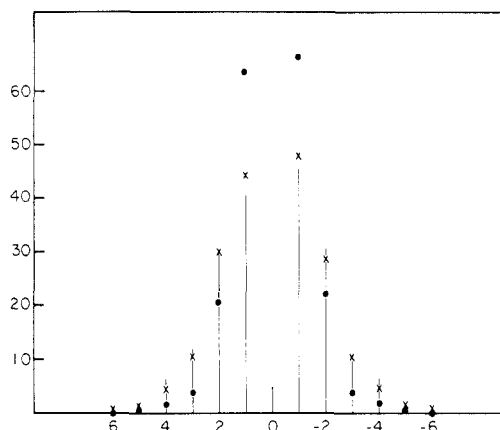


**Figure 10.**  $^1\text{H}$  MAS-NMR (200.27 MHz) spinning sideband peak heights for an orthoclase glass containing 1.5 wt %  $\text{H}_2\text{O}$  at 8.0 kHz spinning speed. Solid lines represent experimental results, and crosses and circles are heights predicted by additive superposition of the experimental spectra of analcite and tremolite (x) and analcite and pyrophyllite (●). The centerbands (not shown) have been scaled to the same heights in all three cases. Note the significantly better fit to the data when the tremolite spectrum is used to simulate the spectrum.

glasses agree very well with simulated spectra obtained by adding the individual spectra of analcite and tremolite in the appropriate proportions (Figure 6a). In contrast, Figure 10 shows that no such agreement can be obtained when pyrophyllite is used instead of tremolite as the standard OH compound. (Also, an analysis of the fractional centerband areas results in much higher OH contents than indicated by the infrared results.) This comparison provides information about the spatial relationships of the OH and  $\text{H}_2\text{O}$  groups.

Studies of hydrogen-containing minerals have shown that homonuclear proton-proton interactions contribute substantially to spinning sideband intensities, if the spinning speeds are comparable to the magnitude of the interactions.<sup>27</sup> In tremolite the OH groups are structurally very isolated from each other (the hydrogen atoms are separated by more than 500 pm),<sup>30</sup> resulting in weak dipolar interactions and low spinning sideband intensities. In contrast, the closest distances between the OH groups in pyrophyllite are significantly shorter (249 pm),<sup>31</sup> resulting in stronger (greater than eightfold) homonuclear dipolar interactions and more intense spinning sidebands.

Thus, the comparison of the experimental spectra with both simulations (Figure 10) strongly suggests that in the glasses the OH groups are structurally very distant from each other and have only weak dipolar couplings. Similarly, there is no evidence for proximity or clustering of OH and  $\text{H}_2\text{O}$  or of two or more  $\text{H}_2\text{O}$  groups. We note, however, that the question of clusters involving  $\text{H}_2\text{O}$  groups may be complicated by the fact that the dipolar interactions between these species are reduced by twofold rotations ("flips") around the bisector axis of the water molecule, such as have been shown to occur in rhyolitic glasses.<sup>21</sup> This behavior might contribute to the observation that even at very high water contents (7.9 wt %  $\text{H}_2\text{O}$ ), where stronger  $^1\text{H}$ - $^1\text{H}$  dipolar interactions are expected purely on statistical grounds, the treatment in terms of noninteracting OH and  $\text{H}_2\text{O}$  species still appears to be valid.

**Chemical Shifts and Hydrogen-Bonding Strengths.** Figure 11 and Table III indicate that magic angle spinning results in substantial line narrowing, the residual line widths amounting to 250 Hz for vitreous silica and 800–1600 Hz for all the other glasses. The question of whether these line widths arise predominantly from insufficient spinning speeds or from a distribution of isotropic chemical shifts can be addressed by measuring the residual centerband line widths as a function of

(a) magnetic field strength: the chemical shift (in Hz) is linearly dependent on the strength of the external magnetic field, whereas

(29) Nayeem, A.; Yesinowski, J. P., submitted for publication.

(30) Hawthorne, F. C.; Grundy, H. D. *Can Mineral.* **1976**, *14*, 334.

(31) Wardle, R.; Brindley, G. W. *Am. Mineral.* **1972**, *57*, 732.

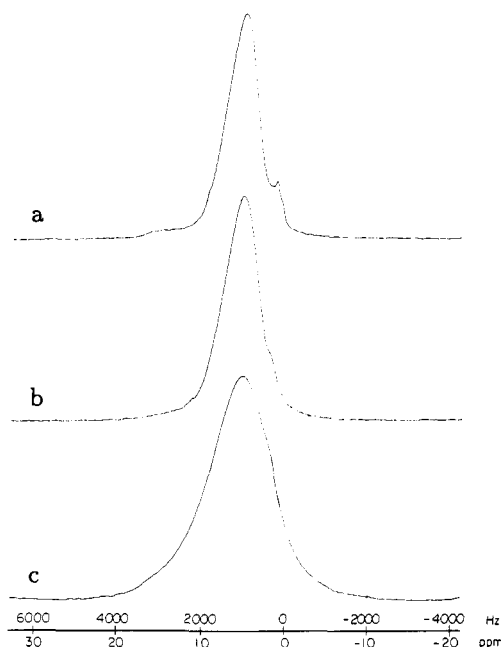


**Figure 11.** 200.27-MHz  $^1\text{H}$  MAS-NMR centerband line shapes for three water-containing glasses: (a) orthoclase glass, containing 1.50 wt %  $\text{H}_2\text{O}$ ; (b) orthoclase glass, containing 2.53 wt %  $\text{H}_2\text{O}$ ; (c) anorthite-silica-wollastonite glass, containing 7.93 wt %  $\text{H}_2\text{O}$ .

dipolar couplings are field-independent;

(b) spinning speed: the residual line width of a sample generally decreases at higher spinning speeds, reaching a plateau value at a spinning speed that depends on the strength of the homonuclear dipolar couplings;

(c) isotopic dilution:<sup>32</sup> isotopic dilution with deuterium greatly reduces the homonuclear  $^1\text{H}$ - $^1\text{H}$  dipolar interactions generally responsible for broadening at lower spinning speeds.

Our experimental results indicate unambiguously that the predominant source of the residual  $^1\text{H}$  MAS-NMR line widths is a distribution of chemical shifts: (a) on increasing the magnetic field strength from 4.7 to 11.7 T the centerband line width (at 8 kHz spinning speed) for both the synthetic and volcanic glasses increases in roughly the same ratio (other line-broadening factors such as field inhomogeneity and angle missetting are small and comparable for both probes); (b) the line width of the centerband is largely independent of the spinning speed within the range 5 kHz  $< \nu_{\text{rot}} < 8$  kHz in both volcanic and synthetic glasses, suggesting that a spinning rate of 5 kHz is sufficiently rapid to average out dipolar coupling contributions; (c) the  $^1\text{H}$  MAS-NMR centerband line width of the residual protons in the hydrated rhyolitic glass in which 85–90% of the dissolved water is  $\text{D}_2\text{O}$  (data not shown) is identical with that observed in corresponding nondeuteriated samples.

Having demonstrated that the  $^1\text{H}$  MAS-NMR line widths of these glasses are due primarily to a distribution of chemical shifts, we next consider the significance of this distribution. Experimental results<sup>14</sup> and theoretical calculations<sup>33</sup> indicate that the  $^1\text{H}$  chemical shifts of oxygen-bound hydrogen depend linearly on the O—H...O distance, an index of the hydrogen-bond strength. Figure 12 shows this correlation using all of the available experimental data,<sup>14,15,34,35</sup> with the exception of older data obtained by less-accurate multiple pulse methods.<sup>14</sup> The data are well-fitted by the equation

$$\delta_{\text{iso}}/\text{ppm} = 79.05 - 0.255d(\text{O—H}\cdots\text{O})/\text{pm}$$

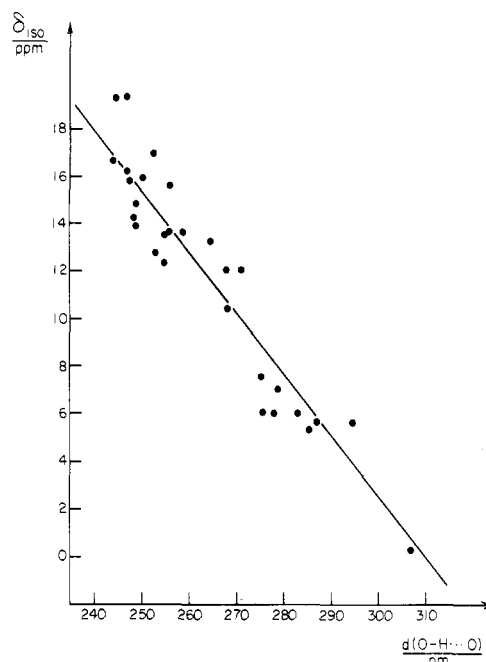


**Figure 12.**  $^1\text{H}$  NMR isotropic chemical shifts vs O—H...O distance, using literature data for crystalline compounds.<sup>15,34,35</sup> The solid line represents the least-squares fit to the data.

From this function we can determine the average O—H...O distance corresponding to the chemical shift of the peak maximum, as well as the shape and width of the O—H...O distance distribution. A slightly discontinuous character in this distribution for most of the synthetic glasses with lower water contents is suggested by the observation of a distinct upfield shoulder in the spectra (see, for instance, Figure 11a). Similar effects have been observed in the  $^1\text{H}$  MAS-NMR spectra of dried silica gel.<sup>17</sup> The fractional area of this shoulder does not appear to depend on the total water content in any systematic fashion and does not offer any means of discriminating between OH and  $\text{H}_2\text{O}$  species. We cannot exclude the possibility that this shoulder is due to surface-adsorbed water. In synthetic glasses with water contents above ca. 5 wt % the line widths tend to increase, possibly reflecting a contribution of homonuclear dipolar interactions. Figure 9a shows that line-broadening effects also result from the presence of iron in the glasses. Although these effects may reflect  $T_2$  or susceptibility broadening, it is also possible that iron may influence the hydrogen-bonding characteristics of water in glasses.

The average O—H...O distance, as determined from the measured isotropic chemical shifts (determined at peak maximum) in conjunction with Figure 12, amounts to 288.5–291.5 pm in the synthetic glasses, 291.5–294.5 pm in the rhyolite glasses, and 297.5 pm in silica glass. These relatively long distances are consistent with weak hydrogen bonding and are in excellent agreement with previous  $^2\text{H}$  NMR data obtained on rhyolite glasses,<sup>21</sup> as well as infrared measurements.<sup>36</sup> The isotropic chemical shifts listed in Table III show that the average O—H...O distances are essentially independent of the overall glass composition over the range we have studied as well as the total water content. Since the percentage of molecular  $\text{H}_2\text{O}$  increases with increasing total water content, the hydrogen-bonding strengths of the OH and  $\text{H}_2\text{O}$  species must be very similar, a conclusion also supported by  $^2\text{H}$  NMR results.<sup>21</sup> The half-height widths of the O—H...O distance distributions, calculated from eq 1 by using the full line widths at half-height  $\Delta\nu_{1/2}$  of the  $^1\text{H}$  MAS NMR centerbands, are listed in Table III. These values contrast with those of ca.  $\pm 20$  pm obtained from infrared studies<sup>36</sup> and  $^2\text{H}$  NMR.<sup>21</sup> We believe that this discrepancy may result from the inadequacy of eq 1 in predicting the dependence of chemical shift on hydrogen-bonding

(32) Eckman, R. J. *Chem. Phys.* **1982**, *76*, 2767.

(33) Rohlifing, C. M.; Allen, L. C.; Ditchfield, R. J. *Chem. Phys.* **1983**, *79*, 4958.

(34) Rosenberger, H.; Grimmer, A. R. *Z. Anorg. Allg. Chem.* **1979**, *448*, 11.

(35) Ratcliffe, C. I.; Ripmeester, J. R.; Tse, J. S. *Chem. Phys. Lett.* **1985**, *120*, 427.

(36) Stolper, E. M.; Aines, R. D.; Rossman, G. R., to be submitted for publication.

length for O—H...O distances greater than 290 pm. By analogy with the results on  $^2\text{H}$  nuclear electric quadrupole coupling constants,<sup>21</sup> the chemical shifts at longer O—H...O distances may depend less strongly on this parameter. However, very few  $^1\text{H}$  NMR chemical shift data have been reported in this range of weak hydrogen-bonding strengths; such a database is needed to determine accurate and reliable distribution functions of hydrogen-bonding strengths in water-containing glasses by NMR methods.

### Conclusions

The present study shows that high-power  $^1\text{H}$  solid-echo and high-speed magic angle spinning (MAS) NMR techniques can provide new insights into the bonding state of the hydrous species in glasses. The most important results are the following.

1. With pyrophyllite or other suitable standards,  $^1\text{H}$  solid echo NMR provides a nondestructive, sensitive method for obtaining absolute water contents in glasses. The quantitation results agree well with those obtained by manometric methods down to a level of ca. 0.1 wt %  $\text{H}_2\text{O}$ ; analysis for lower concentrations would require further reduction of the background signal from the probe. In the presence of iron,  $^1\text{H}$  NMR underestimates the water content to an extent that depends on the iron concentration. It should be possible to use appropriate NMR calibration curves to obtain accurate values from samples with known concentrations of paramagnetic species.

2. High-speed magic angle spinning (at 5–8 kHz) results in substantial line narrowing and characteristic spinning sideband intensity patterns. For water-containing glasses with low levels of paramagnetic ions, the  $^1\text{H}$  MAS-NMR spectra can be simulated as the sum of the individual MAS-NMR spectra of the model compounds tremolite (OH) and analcite ( $\text{H}_2\text{O}$ ). Such simulations, as well as analyses of the fractional centerband areas in the experimental spectra, can be used to obtain the percentages of OH and  $\text{H}_2\text{O}$  in hydrous glasses. The species concentrations

measured by NMR and infrared methods are in good agreement.

3. The agreement of the experimental MAS-NMR spectra with simulations based on the individual spectra of compounds in which the hydrogen-bearing species are structurally isolated (OH in tremolite and  $\text{H}_2\text{O}$  in analcite) indicates that OH or  $\text{H}_2\text{O}$  groups in the glasses are not preferentially clustered.

4. The line shape of the  $^1\text{H}$  MAS-NMR centerbands in these glasses is governed by a continuous distribution of isotropic chemical shifts; since these shifts are correlated with the O—H...O distance, the centerband line shape reflects the distribution function of this distance.

5. The average O—H...O distances in the aluminosilicate glasses studied (290–293 pm) depend very little on the glass composition or the absolute water contents, implying that the hydrogen-bonding characteristics of  $\text{H}_2\text{O}$  and OH species are very similar.

**Acknowledgment.** The NMR experiments were carried out at the Southern California Regional NMR Facility at the California Institute of Technology, supported by NSF grant no. CHE 84-40137. E.M.S. acknowledges additional support by NSF grants EAR 84-17434 and EAR 86-18229. We also thank the donors of The Petroleum Research Fund, administered by the American Chemical Society, for partial support of this research. We thank Professor A. L. Boettcher (University of California, Los Angeles) for assistance with preparation of some of the glasses and Drs. P. Dobson and S. Newman (Division of Geological and Planetary Sciences, California Institute of Technology) for help with the manometric analyses, which were carried out in the laboratory of Prof. S. Epstein. Thanks are also due to Prof. David Live (Chemistry, Emory University) for stimulating discussions, to Dr. G. J. Fine and the Corning Glass Works for providing the anhydrous starting materials for several of the samples investigated, and to Prof. J. R. Holloway (Chemistry, Arizona State University) for providing a water-containing rhyolite glass isotopically diluted with  $\text{D}_2\text{O}$ .

## Nonlinear Dielectric Effect in a Pure and in a Nitrobenzene-Doped Critical Solution of Perfluoromethylcyclohexane–Carbon Tetrachloride

S. J. Rzoska,\* J. Chrapeć, and J. Ziolo

*Institute of Physics, Silesian University, 40-007 Katowice, ul. Uniwersytecka 4, Poland*

*(Received: May 18, 1987; In Final Form: October 15, 1987)*

The influence of additives of high permittivity on the nonlinear dielectric effect in perfluoromethylcyclohexane–carbon tetrachloride solution was studied. In the pure binary solution only a very small critical effect is observed, most probably the smallest of the effects found in solutions of limited miscibility. However, the presence of the additive induced the appearance of a typical strong critical anomaly.

### Introduction

The modern theory of critical phenomena makes it possible to formulate a joint, universal description of the critical anomalies of various physical magnitudes in the vicinity of critical points for systems of varied microscopic types.<sup>1</sup> However, it appears that this success does not yet fully extend to dielectric properties.

Quite recently, a theoretical description together with an experimental verification for electric permittivity was achieved,<sup>2,3</sup>

but the influence of certain significant factors, e.g., measurement field frequency, on the critical effect has not been fully elucidated.<sup>4</sup> The magnitude of electrical conductance also requires further study.<sup>5</sup>

Another property of this type is the nonlinear dielectric effect (NDE) which has been investigated here, i.e., the change in electric permittivity  $\epsilon$  induced by a strong electric field  $E$ .

Tests conducted in pure liquids and in their solutions of limited miscibility have shown that in dipole (polar) liquids the principal contribution to the NDE is most frequently negative<sup>6</sup> and associated with orientation of the dipoles in a strong electric field

(1) Ma Shang-Keng *Modern Theory of Critical Phenomena*; Benjamin: London, 1976.

(2) Goulon, J.; Greffe, J. L.; Oxtoby, D. W. *J. Chem. Phys.* **1979**, *70*, 4741.

(3) Sengers, J. V.; Bedeaux, D.; Mazur, P.; Greer, S. C. *Physica A* **1980**, *104A*, 573.

(4) Thoen, J.; Kindt, R.; Van Dael, W. *Phys. Lett. A* **1980**, *76A*, 445.

(5) Moodithaya, R. Doctor's Thesis, Indian Institute of Sciences, Bangalore, 1987.